Journal of
Composites Science

MDPI

Review

Biochar Derived from Rice by-Products for Arsenic and Chromium Removal by Adsorption: A Review

Stella Chatzimichailidou, Maria Xanthopoulou, Athanasia K. Tolkou * and Ioannis A. Katsoyiannis

Laboratory of Chemical and Environmental Technology, Department of Chemistry, Aristotle University of Thessaloniki, 54124 Thessaloniki, Greece
* Correspondence: tolkatha@chem.auth.gr; Tel.: +30-2310-997997

Abstract: Environmental pollution by arsenic (As) and hexavalent chromium (Cr(VI)) has been one of the most serious environmental problems in recent years around the world. Their presence in water is a result of both natural and anthropogenic activities, and poses serious risks to human health due to their high toxicity. Adsorption is a leading method used to remove arsenic and chromium, with biochar, a carbonaceous pyrolytic product made from various types of biomass, under low oxygen conditions, being one of the most common adsorbents due to its high surface area. Although biochar's ability to immobilize and remove As and Cr(VI) is high, in order to increase the adsorption capacity and nutrient release potential of rice husk biochar, it is essential to select an appropriate pyrolysis and biochar modification technique. Physical or biological activation, steam/gas activation, UV irradiation, magnetization, alkali/acid treatment, and nano-modification are the main modification methods that will be discussed in this review. These modifications have led to multi-fold enhancement in adsorption/reduction capacity of As and Cr(VI), compared with plain biochar. This review provides a recent literature overview of the different biochar modification methods, as well as the factors that influence their capacity to successfully remove As and Cr(VI), along with regeneration potentials.

Keywords: arsenic adsorption; chromium adsorption; biochar; rice husk; rice straw

Citation: Chatzimichailidou, S.; Xanthopoulou, M.; Tolkou, A.K.; Katsoyiannis, I.A. Biochar Derived from Rice by-Products for Arsenic and Chromium Removal by Adsorption: A Review. *J. Compos. Sci.* **2023**, *7*, 59. https://doi.org/10.3390/jcs7020059

Academic Editors: Ahmed Koubaa, Mohamed Ragoubi and Frédéric Becquart

Received: 26 December 2022
Revised: 10 January 2023
Accepted: 1 February 2023
Published: 4 February 2023

1. Introduction

Worldwide, millions of people have no access to safe drinking water and are exposed to water contaminated with arsenic and chromium, mostly in Southeast Asia and in Europe [1–3], while in many cases, arsenic and chromate have been found to occur simultaneously in water or wastewater sources [4,5].

Arsenic (As) is found in almost all environmental matrices, and is one of the most critical natural contaminants of global concern due to its highly toxic effects on different life forms, including humans. Arsenic ranks 20th in the earth's crust, 14th in seawater, and 12th in the human body in terms of abundance [6]. Additionally, it ranks number one in the USA.'s Agency for Toxic Substances and Disease Registry's Priority List of Hazardous Substances [7]. Arsenic usually originates in groundwater and is one of the foremost contaminants. Less than half the world has a likelihood of less than 20% of encountering groundwater with less than 10 μg/L of arsenic (Figure 1) [8], which is the limit in drinking water set by the Drinking Water Directive 98/83/EC [9].

Arsenic appears to be thermodynamically stable in the chemical form of arsenate ion in water. At medium or high redox potentials, arsenic can be stabilized as pentavalent (arsenate) oxyanion, H_3AsO_4, $H_2AsO_4^-$, $HAsO_4^{-2}$ and AsO_4^{-3}, while under reducing conditions and lower redox potential, the trivalent arsenite species (H_3AsO_3) are more prominent. Figure 2 shows the different species of arsenic under different redox and pH conditions [10].

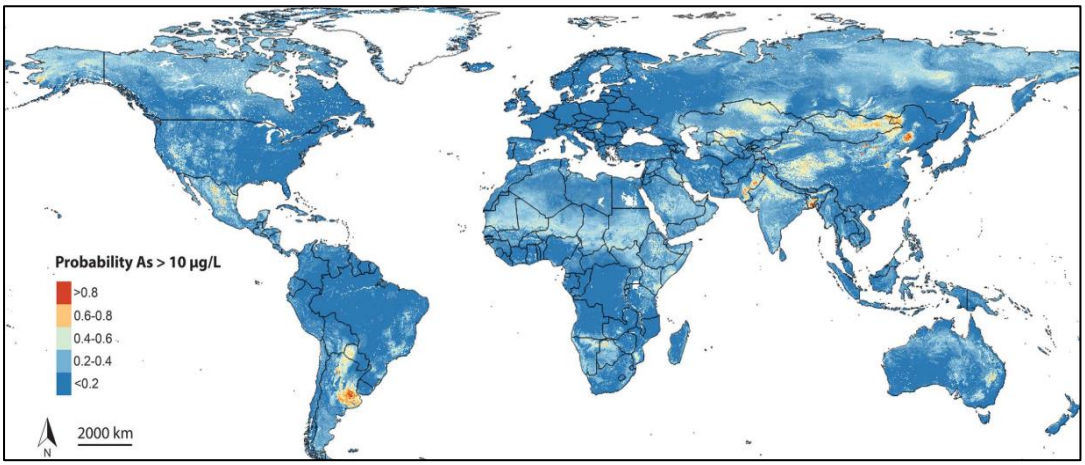

Figure 1. Modeled probability of arsenic concentration in groundwater exceeding 10 µg/L for the entire globe [8].

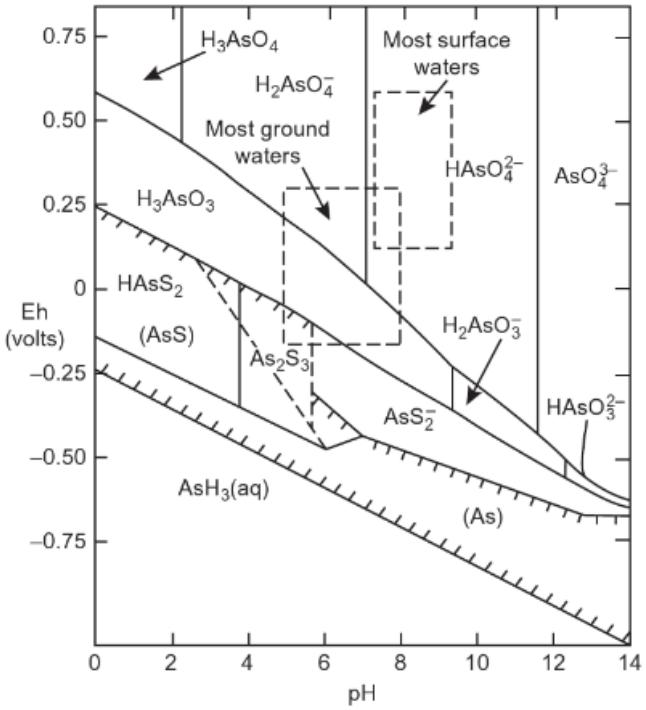

Figure 2. Eh–pH diagram of aqueous arsenic species in water at 25 °C and 1 bar total pressure [10].

Another major contamination problem is the presence of Cr(VI) in groundwaters worldwide. Chromium (Cr) can originate from both natural and anthropogenic sources, such as volcanic eruptions, emissions from fossil fuel combustion and tannery wastewater discharge. Its toxicity varies according to its oxidation state, which is controlled by the physicochemical properties of the soil. It can be harmful or beneficial to living organisms depending on its oxidation state, which can vary from −2 to +6. The most common and stable forms of chromium in the environment are the trivalent (Cr(III)) ($Cr(OH)_3$) and hexavalent (Cr(VI)) (i.e., CrO_4^{2-} or $Cr_2O_7^{2-}$). Chromium(III) is commonly encountered as insoluble chelates or precipitates. Chromium (VI) is one of the most well-known carcinogenic elements, and can have catastrophic effects on the blood system, liver, kidney, and the gastrointestinal and immune systems [11]. The reduction of Cr(VI) to the less toxic Cr(III) is important for the remediation of soils and waters contaminated with Cr(VI) [12]. The United States Environmental Protection Agency (EPA) has a drinking water standard of 100 µg/L for total chromium [13], and the respective World Health Organization's (WHO)

permissible limit is 50 µg/L [14]. The European Commission decided to reduce their allowable value by 50% of WHO's limit, i.e., to 25 µg/L, and the new limit will have to be complied with by 2036.

Worldwide, a large amount of research on arsenic removal technologies has been carried out to increase arsenic uptake from natural waters. Adsorption is one of the most popular methodologies to remove arsenic and associated heavy metals from water and wastewater. Adsorption is efficient and economically feasible in comparison with other arsenic removal technologies such as ion exchange, phytoremediation, chemical precipitation, electrocoagulation and membrane technology, and has >95% quantitative efficiencies reported for arsenite and arsenate remediation [15]. A large number of adsorbents have been successfully applied for arsenic remediation including natural and modified clays, minerals, and other geological materials such as zeolite [16], silica [17], goethite [18], calcite [19], activated carbons [20,21], biosorbents [22], biochars [23], and synthetic adsorbents such as hierarchically porous CeO_2–ZrO_2, nanospheres, molecularly imprinted polymers, and the Fe(III)-H_2O_2 system [24–28].

In addition, a wide range of technologies has emerged for the treatment of Cr-contaminated environments (Table 1). The approaches to remediate Cr may be on-site or off-site, in situ or ex situ, for example, soil encapsulation, immobilization, mobilization, soil washing, electrokinetic, biosorption, and biotransformation. Each method displays specific benefits and disadvantages. Physical remediation technologies are simple and rapid, but incur a high cost due to high energy consumption [29]. Chemical remediation technologies exhibit high removal efficiency, however, they can potentially cause nutrient loss in soil. Biological remediation methods are much greener, but they require time-consuming pre-treatment to be effective [30].

Of the above, using immobilizing agents is the most popular method to stabilize Cr in soil or remove it by adsorption from water [31,32]. Chemical immobilization is an inexpensive and environmentally friendly way to holistically remediate heavy metals, especially in large-scale application [33]. Biochar has emerged as a green and low-cost adsorbent for treating Cr pollution in soil and water [29]. Biochar is a product of thermal decomposition of various types of biomass (rice husk, wood, straw, bamboo, or fruit peel [34] under limited oxygen and a wide range of temperatures (<700 °C)) [35]. It is often used as a soil pollutant adsorbent due to its special physical and chemical properties.

Table 1. Cr(VI) pollution treatment methods [36].

Method	Advantages	Disadvantages
Physico-chemical methods		
Membrane filtration	High removal capacity. Requires less physical space. Low generation of solid wastes. Good performance at lower pressure and high rejection rate.	Sludge generation. High cost. Specific range of pH. Membrane fouling. Bacteria easily damage the filter. Performance depends on the material composition and pore size of the filters. Multi-component pollutants lead to low flow rates and bad performance.
Coagulation/flocculation	Settling of solutions requires less time. Higher capacity for dewatering. Low cost.	Sludge generation, high chemical consumption. High cost because of the need to clean the generated sludge.
Solvent extraction	Rapid recovery of metal. Short duration.	Need for specific solvents. High cost.

Table 1. *Cont.*

Method	Advantages	Disadvantages
Physico-chemical methods		
Ion exchange	Good removal efficiency, achieves high selection. Less production of sludge and relatively low emissions. Rapid procedures and regeneration options.	Chromium ions removal is problematic due to multi-components in soil. Chemical reagents used in regeneration process generate secondary pollutants. Solids foul the resin. High-cost investment required to remove low concentration metal from wastewater.
Chemical precipitation	Simple and safe design and operation. Low energy consumption, low cost.	Generation of toxic sludge derived from the chemicals used for the precipitation. Massive generation of sludge that exceeds the disposal standards.
Adsorption	Simple design. Good performance. Regeneration and recyclability options. Low sensitivity to high concentration of chromium. Effective removal of low concentrations. Zero-cost and low-cost precursor.	Regeneration of adsorbate from the adsorbent. Activation and modification of the materials has a high cost. Disposal problems for loaded absorbents.
Electro-chemical methods		
Electrocoagulation	Simple method capable of treating chromium co-existing with other pollutants.	Electrode requirements, unorganized design. Electrode corrosion problems, high cost. Requirement of electricity for large scale application.
Electrochemical reduction	Low cost, no need for reagents, effective with high capacity.	High cost related to the type of electrode and its characteristics. Need for further separation of Cr(III).
Electrosorption	High specific surface area with mesopores and micropores increasing the removal of chromium ions. Minimum energy consumption, low cost. Regeneration options. Operates at low pressure and within small space.	The structure of electrical double-layer superimposed within the electrode affects the adsorption performance for chromium.
Electrodialysis	Low energy consumption, low cost.	Limitation associated with electrode costs and maintenance costs of membrane.
Biological methods		
Biosorption and bioaccumulation	Green technology. Various types of biomass can be used.	High chromium concentrations poison live microbes. Media requirements. Fluctuating performance. Complex mechanisms. Biosorbent regeneration requires chemical usage. Biosorbent loaded with chromium.
Advanced methods		
Nanotechnology	Various functional nanomaterials available with excellent removal rates. Small generation of waste and specific chromium removal.	Residual effects of nanoparticles after application in the environment.

Biochar has proven to be an efficient material regarding the removal of heavy metals from water, and, therefore, biochar-based technologies are a promising tool for water remediation technologies [37]. Solid carbonaceous biochar is obtained from biomass pyrolysis

in the absence of oxygen [38]. Among the properties of biochar are high surface area, resistance to degradation, porosity, and surface-oxygenated functional groups [39]. Oxygen-rich functional groups charge biochar surfaces negatively. Consequently, extensive removal of anions and oxyanions occurs at low pH (<4.0), where biochar's surface functional groups undergo protonation [40].

Waste-based biochar is considered to be a low-cost and environmentally friendly material. The yield of biochar and its structures are dependent on the thermochemical processes, operating conditions, and feedstock. Rice husk (RH) is an affordable and sustainable feedstock to be transformed into biochar. Rice husk is a natural organic–inorganic composite containing lignin, cellulose, hemicelluloses and silicon dioxide (SiO_2) [41]. It has been established that the low-temperature-derived biochars from slow pyrolysis lead to low hydrophobicity and aromaticity but high surface acidity and polarity. When high temperature is applied during the production of biochar, the pore size enlarges and the wall between adjacent pores is destroyed, which explains the diminishing pore structure of biochar. The presence of inorganic material from feedstock ash has also been observed on RH biochar surface, which could partially fill or block the porosity [42].

The aim of this review is to provide a recent literature overview of the different biochar modification methods, as well as of the factors that influence their capacity to successfully remove As and Cr(VI).

2. Biochar for Arsenic (As) Removal

The aim of this review is to analyze recent literature related to the application of biochar derived from rice by-products, especially from rice husk, for the removal of As(III) and As(V) from water. The main type of arsenic in water is in the form of oxyanions, and as the surface of unmodified biochars is generally negatively charged, these are less effective sorbents for As species. This is due to static repulsion between the As oxyanions and the negatively-charged biochar surface. Biochar composites are typically formed by impregnation of biochar with metal oxides in order to acquire a positive charge on the biochar's surface. The modification procedure can be performed by pre-pyrolysis or post-pyrolysis treatments to enhance the physicochemical properties and surface morphologies of biochar. Table 2 includes As sorption studies for pristine and modified biochar adsorbents derived from rice by-products, mostly rice husk and rice straw feedstock.

Table 2. Studies on As removal via adsorption on rice husk and rice straw derived biochar.

Material	Adsorption Capacity, Qm (mg/g)	pH	Biochar Dose (g/L)	Initial Concentration (mg/L)	Reference
Commercial rice husk biochar	19.3 As(III) 7.1 As(V)	8 6	5	3–300	[43]
Fe-coated rice husk biochar	31 As(III) 17 As(V)	8 6	5	3–300	[43]
Rice husk biochar (RH)	0.35 As(V)	9.5	2	0–200	[44]
Rice husk biochar (BC-RH)	0.00259 As(V)	6.7–7	8	0.09	[45]
RH–Ca^{2+} biochar	1 As(V)	10.8	8	0.8	[46]
RH–Fe^{0} biochar	-	7.4 7	16 16	0.8	[46]
RH–Fe^{3+} biochar	-	2.4 6.8	1 16	0.8	[46]
Fe(III)-modified rice straw biochar (RS)	27 As(V)	5	1	0.0011–0.0127	[47]
Rice straw biochar	0.552 As(V) 0.447 As(III)	6 2	4	1–50	[48]
Red-mud-modified rice straw biochar (RM-BC)	5.92 As(V) 0.52 As(III)	6 2	4	1–50	[48]

Table 2. *Cont.*

Material	Adsorption Capacity, Qm (mg/g)	pH	Biochar Dose (g/L)	Initial Concentration (mg/L)	Reference
Biochar–Fe/ Biochar–Cu (3:1)	20.32 As(V)	7	10	0.5–128	[49]
Magnetic biochar (mBC)	4.59 As(V)	5	2	1–100	[50]
Al-magnetic biochar	15.75 As(V)	5	2	1–100	[50]
Mg-magnetic biochar	16.66 As(V)	5	2	1–100	[50]
MgAl-magnetic biochar	34.45 As(V)	5	2	1–100	[50]
Rice husk biochar, BC	0.14 As(III) 0.42 As(V)	7	2	10	[51]
MnO_2/rice husk biochar composite, MBC-100	1.88 As(III) 2.16 As(V)	7	2	10	[51]
Fe–Al bimetallic oxide/biochar	8.69 As(III)	5.5	-	2.5–20	[37]

2.1. Sorption Studies of Biochar Derived from Rice by-Products for As Remediation

2.1.1. Fe-Coated Rice Husk Biochar

Samsuri et al. [43] studied the adsorption capacity of a commercially produced rice husk biochar (RHB) for As(III) and As(V) [43]. The RHB's surface modification was performed by coating Fe(III) on it. The Fe-coated RHB was capable of adsorbing As(III) and As(V) from aqueous solutions with the adsorption of As(III) higher than As(V), while the use of Fe-coated biochar increased the adsorption capacity for both As(III) and As(V). The amount of As(III) adsorbed increased with the increase of the solution pH for all the sorbents, and the maximum adsorption occurred at pH 8 and 9. By increasing the solution pH to 6, the amount of As(V) adsorbed also increased for all the sorbents, but after pH 7 it decreased. The isotherm adsorption data were fitted to the Langmuir adsorption model. The maximum adsorption capacity, q_{max}, for As(III) was 19.3 mg/g, while coating the biochar with Fe(III) increased the q_{max} for As(III) to 30.7 mg/g. The q_{max} for As(V) was only 7.1 mg/g, while the q_{max} of the Fe-coated RHB for As(V) increased to 16.4 mg/g. The formation of surface complexes between As(III) and As(V) and the functional groups of RHB could be the main mechanism for the adsorption of As(III) and As(V), while the relative possible mechanism of As(III) and As(V) onto the Fe-coated RHB is their interactions with FeOH and $FeOH^{2+}$ groups [43].

2.1.2. Rice Husk Biochar (RH)

Norazlina et al. [44] produced and studied a biochar material derived from rice husk from the BERNAS (Malaysian National Rice Agency) rice mill in Tanjung Karang, Selangor [44]. The chemical and physical characteristics for RH biochar are presented in Table 3. The RH biochar pH value was 9, while the EC value was 2.90 dS/m, and the material contained a significant amount of nutrients with high levels of potassium. The RH biochar also contained minor levels of arsenic and cadmium (1.15–0.45 mg/kg). Morphologically, the pores on the RH biochar were not well shaped and small pores were detected on the rough surface of the RH biochar. The internal surface area of biochar was referred to as micropore area, and the average pore diameter was in the range of mesopores diameters.

The alkaline properties of the biochar increased the solution pH, which caused a decrease in arsenic solubility due to precipitation. The adsorption isotherm study was conducted for a dose of 2 g of biochar, the data were fitted to the Langmuir adsorption model and the maximum adsorption capacity (q_{max}) of RH biochar for As(V) was 0.352 mg/g [44].

Table 3. The chemical and physical properties of rice-husk-derived biochar [44].

pH (1:2.5 H_2O)	10.24
EC (dS/m)	2.90
Total carbon %	7.78
Total nitrogen %	0.23
Phosphorus %	0.36
Potassium %	0.72
Calcium %	0.02
Magnesium %	0.08
Arsenic (mg/g)	0.55
Cadmium (mg/g)	0.45
Surface area (m^2/g)	23.22
Micropore volume (cm^3/g)	0.009
Internal surface area (m^2/g)	1.41
Average pore diameter (nm)	4.34

2.1.3. Rice Husk Biochar (BC-RH)

Agrafioti et al. [45] synthesized biochar from rice husk that was collected from a rice mill located in northern Greece [45]. An adsorption kinetic study was performed for the initial concentration of 90 μg/L As(V) with 4 g/L of adsorbent. The kinetic data fitted well with the pseudo-second order kinetic model. According to the pseudo-second order kinetic model, the reaction rate is based on the assumption that the rate-limiting step is chemical sorption or chemisorption, and predicts the behavior over the whole range of adsorption. An adsorption equilibrium study took place for varying concentrations of metals (90–850 μg/L) and adsorbents (1–16 g/L). The adsorption isotherm data of As(V) fitted the Freundlich model while the Langmuir model failed to describe the obtained data due to the heterogeneous surface of the initial feedstocks and, thus, of the produced biochar. The maximum As(V) removal achieved was 25% for BC-RH. The low ash content of BC-RH (∼17%), as well as its high ash content in SiO_2 (81.3% w/w of dry matter) and low content in Ca, Fe, and Al oxides (<1.3% w/w) could explain its inefficiency in removing As(V) from the aqueous solution [45].

2.1.4. Ca- and Fe-Modified Biochars

Agrafioti et al. [46] studied the arsenic adsorption capacity of calcium- and iron-modified biochars (RH–Ca^{2+} biochar, RH–Fe^0 biochar, RH–Fe^{3+} biochar) derived from rice husk that was collected from a rice mill located in northern Greece, which they produced by pretreating prior to pyrolysis with Ca^{2+}, Fe^0 and Fe^{3+} [46]. Equilibrium experiments were conducted for the initial concentration of 800 μg/L As(V) with varying concentrations of adsorbents (1–16 g/L). They conducted two sets of experiments, using 11.4 g Ca or Fe/100 g biomass of rice husk for the first set, and 2.3 g Fe/100 g biomass of rice husk for the second set. For the first set of experiments, the data for As(V) adsorption on RH–Ca^{2+} fitted best to the Freundlich model. However, As(V) adsorption data for RH–Fe^{3+} biochar could not be fitted with an isotherm model as all the adsorbent doses that examined the removal rates were higher than 97%. For the second set of experiments, the Freundlich model also fitted the data better than the Langmuir model for the RH–Fe^{3+} biochar, while for both sets of experiments, the data obtained for the biochar RH–Fe^0 did not fit any of the tested models. Biochar modified with 11.4% w/w Fe or Ca, derived from rice husk, was very effective in removing As(V) from aqueous solutions, at removal rates of >95%, except for the case of RH–Fe^0 biochar, for which the removal rate was 58%. For the RH–Fe^{3+} biochar, the removal rate was 72% for total As(V), for the maximum adsorbate dose applied

(16 g/L) [46]. A comparison of the removal rate for all Ca- and Fe-modified biochars, as well as the unmodified biochar, is presented in Table 4.

Table 4. Arsenic removal efficiency for unmodified, Ca- and Fe-modified, rice husk biochar [46].

Initial As(V) Concentration (μg/L)	Modification	pH	Biochar	Maximum Removal %	Optimum Adsorbent Dose (g/L)
800	11.4% Ca or Fe	10.8	RH–Ca^{2+}	>95	8
		7.4	RH–Fe^{0}	58	16
		2.4	RH–Fe^{3+}	>95	1
	2.3% Fe	7	RH–Fe^{0}	50	16
		6.8	RH–Fe^{3+}	72	16
90	Unmodified biochar	6.7–7	RH	25	8

2.1.5. Fe (III)-Modified Rice Straw Biochar (RS)

Pan et al. produced biochar from rice straw that was collected from Nanjing, China [47]. A porous structure was formed prior to Fe(III) modification of the biochar. Subsequently, Fe(II) particles adhered to the surface of the biochar, forming iron oxides on it. The functional groups on the biochar were covered by Fe-hydroxide during the modification process, which reduced the negative charge on the biochar. Additionally, Fe(III)-modified biochar acquired a positive charge as a result of the protonation of the hydroxyl on Fe-hydroxide. The arsenate anion was more effectively adsorbed from the aqueous solution onto the biochar surface due to the changes in biochar surface charges caused by Fe(III) alteration.

As(V) adsorption was studied for initial As(V) concentrations of 0.0011–0.0127 mg/L and 1 g/L adsorbent at pH 5. The Langmuir isotherm model fitted the adsorption data better. As(V) adsorption by the unmodified and modified biochar increased as the As(V) concentration in the equilibrium solution increased. The unmodified biochar, however, only adsorbed a very little amount of As(V) (0.19–3.86 g/kg). The pH enhanced and lowered the As(V) adsorption capabilities of the Fe(III)-modified biochar, as well as its surface charge. As(V) adsorbed by the Fe(III)-modified biochar primarily interacted with Fe-hydroxides and created inner-sphere complexes with the Fe-hydroxides that had been produced on the biochar surfaces [47].

2.1.6. Red-Mud-Modified Biochar (RM-BC)

Wu et al. studied the arsenic, As(III) and As(V), adsorption capacity of red-mud-modified biochar (RM-BC) produced from rice straw [48]. RM-BC was prepared by mixing the rice straw biomass with red mud suspensions and the mixture was filtered and pyrolyzed to obtain the composite material. To investigate As adsorption mechanisms, adsorption kinetic studies were conducted for 10 mg/L As(III) and As(V) solutions with a dose of 4 g/L adsorbent at pH 6 and 2. The data were considerably more conformed to the pseudo-second order model for unmodified biochar and RM-BC adsorbed As(V), and for As(III) adsorption on RM-BC, the Elovich model agreed with the data more precisely. Compared with unmodified biochar (BC), RM-BC demonstrated a higher sorption capacity for As. At different As levels (1–50 mg/L As(V)/As(III)), adsorption equilibrium isotherms for As adsorption on RM-BC and BC were evaluated. The Langmuir adsorption mechanism was followed by both BC and RM-BC. The calculated Langmuir maximum adsorption capacity (q_{max}) of RM-BC for As(V) and As(III) was 5923.8 and 520.0 μg/g, respectively, while the q_{max} of BC for As(V) and As(III) was 552.0 and 447.6 μg/g, respectively [48].

2.1.7. Fe and Cu Biochar Composites

Biochar materials modified with iron and copper oxide nanoparticles were obtained by treating rice-husk-derived biochar, after pyrolysis, with $FeCl_3$ and $CuCl_2$ and their subsequent reaction with NaOH solution [49]. The adsorption capacity was studied for the

mixture 3:1 of biochar–Fe and biochar–Cu for solution containing 1:1 mixture of arsenite and arsenate, 0.5–128 mg/L concentration, and 10 g of adsorption material. The composite adsorbent removal rate for both As(III) and As(V) was above 95%, depending on contact time, pH, and co-existing ions in the solution. The studies indicated that the CuO nanoparticles of the composite facilitated the oxidation of As(III) to As(V) before adsorption and exhibited an additional advantage compared with other reported techniques where the pre-oxidation step of trivalent arsenic to pentavalent is required in order to enhance the removal efficiency. The arsenic adsorption data fitted better to the pseudo-second order kinetic model and the Freundlich isotherm model. The maximum adsorption capacity (q_{max}) of the composite mixture was 20.32 mg/g. Arsenic maximum adsorption rate increased to >95% at pH 7.0, while it decreased to 80% and 72% at pH 6.0 and 8.0, respectively. The surface charge of the composite adsorbents and the ionization potential of the arsenic species were both influenced by the pH of the solution. The mechanism of arsenic removal, based on the kinetic and isotherm studies, involved two steps. Firstly, As(III) was oxidized to As(V) in the presence of O_2 and CuO nanoparticles and then the adsorption of As(V) occurred onto the Fe_2O_3 and CuO nanoparticles attached on the biochar surface [49].

2.1.8. Al- and/or Mg-Oxide-Modified Magnetic Biochar Adsorbents

Magnetic biochar (mBCs) adsorbents were synthesized by pretreating rice husk with $FeCl_3$, $AlCl_3$ and $MgCl_2$ solutions, and then pyrolyzed to obtain biochar materials [50]. The four magnetic biochar materials (mBCs) that were tested for their arsenic adsorption capacity were the pristine magnetic biochar, and three aluminum (Al) and/or magnesium (Mg) oxide-impregnated magnetic biochar adsorbents, Al-mBC, Mg-mBC, and MgAl-mBC. An adsorption isotherm study was performed for 1–100 mg/L As(V) initial concentrations and 2 g/L of adsorbent at pH 5.0. The obtained data fitted well to both Freundlich and Langmuir models, so the adsorption occurred on both homogeneous and heterogeneous surface sites. Among all mBCs, the MgAl-mBC adsorbent was found to be the most efficient for As(V) removal. The maximum As(V) adsorption capacity of MgAl-mBC was 34.45 mg/g.

The maximum As(V) adsorption occurred at pH 4 for all mBCs adsorbents. The As(V) removal rates were found to be 39.8, 27.1, and 19.8% for MgAl-mBC, Mg-mBC, and Al-mBC, respectively, compared with the pristine mBC. The adsorption of As(V) on mBC depends on ionic strength, which means that the As anions tend to form outer-sphere surface complexes. As(V) adsorption on Mg-mBC showed ionic strength dependency that was weak, which implied that strong surface complexes were formed. The As(V) adsorption capacity of the MgAl-mBC at 10 mg/L initial concentration decreased as pH increased from 4 to 11. This behavior was suggestive of the inner-sphere adsorption mechanism [50].

2.1.9. MnO_2/Rice Husk Biochar

Cuong et al. synthesized a MnO_2/rice husk biochar composite, MBC, for arsenic water remediation [51]. Rice husk biochar was purchased from Mu-En Farm, Xinshi Dist., Tainan City, Taiwan, and it was treated with manganese(II) acetate tetrahydrate solution in order to obtain the MnO_2 composite material. The study of the effect of the initial concentration on the arsenic adsorption capacity was conducted for pristine biochar and MBC-100 at pH 7, and the adsorption capacity increased on increasing the initial arsenic concentration. This finding might be explained by the concentration gradient driving force for ion transport that results in in greater contact between arsenic ions and the material surface. The As(III) and As(V) adsorption capacities of MBC-100 were 1.88 and 2.16 mg/g, respectively, while those of pristine biochar were 0.14 and 0.42 mg/g, respectively, for the 10 mg/L arsenic initial concentration. The higher values of adsorption capacities by MBC-100 were attributed to the higher porosity and the presence of MnO_2. The As(III, V) removal efficiency was higher at pH 4 and lower at pH 10, for both materials.

The arsenic removal efficiency of MBC-100 was also tested for simulated groundwater containing an arsenic concentration of 100 μg/L (90% As(III) and 10% As(V)) and

90 mg/L NaCl. Arsenic concentration decreased considerably in the first five minutes (77.5% eliminated), and then progressively until 120 min. Only 5.9% of As(III) remained in solution under neutral conditions, proving that MBC-100 has a strong oxidizing potential for As(III). The generated As(V) formed surface complexions with Mn–OH on MnO_2 and manganese arsenate precipitated with reduced Mn(II). MBC-100 showed great arsenic removal efficiency of 94.6% with simulated groundwater and the remaining concentration of arsenic was as low as the 10 µg/L WHO guideline [51].

2.1.10. Fe–Al Bimetallic Oxide/Biochar

A magnetic, eco-friendly Fe–Al bimetallic oxide/biochar composite was studied for As(III) adsorption by Liu et al. [37]. The composite biochar was synthesized by treating rice husk biochar with $FeCl_3$ and $AlCl_3$ solution. Batch adsorption experiments were carried out for different initial concentrations (2.5–20 mg/L) of arsenic solution. While the adsorption capacity declined as the pH range increased from approximately 5.4 to 11, the adsorption capacity increased as the pH range increased from approximately 3.1 to 5.5. Since the adsorbent did not achieve saturation at low concentrations, the adsorption capacity of the 10 mg/L initial arsenic concentration was larger than the 5 mg/L initial concentration at the same pH. The adsorption capacities for the initial concentrations of 2.5–20 mg/L were studied at 30, 45 and 60 °C. The greatest adsorption capacity at 60 °C was achieved with less than 2 mg/L as equilibrium concentration. Moreover, there was negligible difference between the adsorption capacity at 30 °C and 45 °C. It was possible that at lower concentrations and temperatures up to 60 °C, the reaction was stronger. However, when the equilibrium concentration reached about 15 mg/L, the adsorption capacity at 30 °C was greater than that at 60 °C. This suggested that even at higher initial concentrations, arsenic may still be absorbed by the produced material at high temperatures. The results fitted better with the Freundlich model, suggesting that the adsorption process may be occurring on the heterogeneous surface layer that the loaded bimetallic oxides have caused to form.

2.2. Discussion

Biochar is a material that can be utilized as an arsenic adsorbent, depending on the pyrolytic temperature, as sorption is better accomplished by low-temperature biochars than by high-temperature biochars. The pyrolytic temperature, residence duration, feedstock, and pyrolysis technology all have an impact on the characteristics of arsenic adsorption onto biochar. Additionally, adsorbate and adsorbent dosage, solution pH, and equilibration time all have an impact on the assimilation of As. Enhancing As sorption by changing the surface of the biochar has received much attention. Iron has been modified using a variety of coatings, including nano zero valent iron [46] and other materials such as Al and Mn [37,50,51]. Electrostatic attraction, ion-exchange, physical adsorption, and chemical bonding (complexation and/or precipitation) are the most common As adsorption mechanisms onto biochar. For the mentioned materials, the adsorption mechanism is best described by the pseudo-second order kinetic model and both the Freundlich [37,45,46,49,50] and Langmuir [43,44,47–50] isotherm models. It seems that the origin and special characteristics of the feedstock as well as the modification method of biochar have an impact on the surface heterogenicity of the material.

According to some research, modified biochars, i.e., Fe-coated rice husk biochar [43], Fe(III)-modified rice straw biochar (RS) [47], biochar–Fe/biochar–Cu (3:1) [49], and MgAl-magnetic biochar [50], are more efficient than pristine biochar at removing As from water. The most promising functional groups in the modified biochars, which are able to remove comparatively more As from solutions, may be the reason for their improved As retention ability. Synthesis of modified biochar, derived from rice by-products that have been presented above, have been reported as either pre- or post-treatment of biochar pyrolysis. Concerning the efficiency of all mentioned composite materials, as presented in Table 2, it

seems that for both As(III) and As(V) adsorption, the post-pyrolysis treatment of biochar results in materials with higher capacity [43,47,49].

Biochar may be utilized in water treatment for oxyanions and metalloids with modifications that increase its surface area and mechanical qualities. An interesting area for future research is organic arsenic elimination using biochar, in which no studies have yet focused.

2.3. Improved As Adsorption Capacity of Biochar

Modified biochar is regarded as a novel way to provide surface characteristics that encourage As adsorption. As mentioned previously, enhanced As sorption capacity of biochar can be achieved by low temperature pyrolysis technique. More specifically, the adsorption capacity is related to high specific surface area, and the surface area of biochar depends on the pyrolysis temperature. Lower pyrolysis temperature results in higher biochar yield, while higher temperatures result in greater porosity and the removal of oxygenated functional groups [52]. Biochar synthesized at low temperatures is preferred for As removal because it contains more oxygenated functional groups, that could be used for further modification.

An alternative biochar modification technique could be microwave pyrolysis. Microwave pyrolysis is considered to be a cost-effective technique compared with conventional pyrolysis as it is a cleaner and more energy-saving procedure. The main feature of the use of microwaves is the reduction in pyrolysis time by eliminating the temperature gradient that is created in conventional pyrolysis, as no direct contact of the radiation source with the sample is taking place. The difference in the heating process of the biomass could result in a biochar material with better surface and porosity properties that could be beneficial for As sorption [52].

Methods that include strong acids, strong bases, metallic iron and iron ion, metal oxides, and metal/nanoparticle composites, can be used for the surface modification of biochar. Strong acids such H_2SO_4 can be used for surface activation enhancing acidic functional groups, while strong bases such as KOH can be used for reduced particle size, higher surface area and porosity and for electron donor–acceptor interactions with negatively charged As species. The impregnation of biochar with iron such as Fe(0) or Fe(III) introduces As–Fe co-precipitation and As diffusion within particles and anion exchange, as inner-sphere complexation with Fe and strong electrostatic attraction, respectively. Concerning the use of metal oxides, FeO introduces a redox reaction between Fe(II) and As, Fe_2O_3 particles on the surface function as the adsorption sites through electrostatic interaction with As species, MnO_2 oxidizes As(III) to As(V) enhancing the As(III) adsorption, ZnO enhances specific surface area and surface porosity, and CuO offers reusability and stability. Metal/nanoparticle composites such as Ca or Mn combined with Fe nanoparticles also can introduce surface adsorption/oxidation properties, increased surface area, electrostatic interaction forces and surface complexation reactions [53].

3. Biochar for Chromium (Cr(VI)) Removal

3.1. Biochar for the Remediation of Soil Cr Pollution

There has been a wide investigation for the scavenging effect of biochar against Cr(VI) due to the fact that biochar is a proton donor for the reduction of Cr(VI) to Cr(III) [54]. Biomass used for the production of biochar, which can include sludge, agricultural residues, wood and manure, plays an insignificant role in affecting the Cr immobilization potential of each biochar. Nonetheless, the biochar application rate is positively correlated ($r = 0.28$, $p < 0.05$, Table 5) with the Cr immobilization ability, and raising the application rate up to 130 t/ha expanded the immobilization efficiency up to 84%.

The Cr content of pristine biochar is thought to be one of the reasons for the low immobilization capacity of Cr in soils, as is shown by their negative correlation ($r = -0.42$, $p < 0.05$, Table 5). Therefore, it is necessary to establish the ideal conditions for biochar production, in order to achieve the desirable properties.

Table 5. Exponential relationships between Cr immobilization efficiency (Y) and biochar production conditions, biochar properties, and soil properties (X), developed through exponential regression analysis.

Parameter (X)	Equation	*r*	*p*
Pyrolysis temperature (°C)	Y = 44.50 + 0.02X	0.14	<0.05
Pyrolysis residence time (min)	Y = 32.96 − 0.11X	−0.39	NS
Biochar pH	Y = −50.45 + 11.53X	0.39	<0.05
Biochar EC (dS/m)	Y = 18.02 + 0.05X	0.41	NS
Biochar ash (%)	Y = 0.74 + 0.52X	0.74	<0.01
Biochar C (%)	Y = 21.42 + 0.85X	0.46	<0.05
Biochar Cr (%)	Y = 29.43 − 0.28X	−0.42	<0.05
Biochar application rate (t/ha)	Y = 44.73 + 0.25X	0.28	<0.05
Soil pH	Y = −116.74 + 23.09X	0.65	<0.05
Soil organic C (%)	Y = −283.63 + 149.40X	0.56	NS

Cr immobilization efficiency was increased to 73% when increasing pyrolysis temperature to 700–900 °C through the thermochemical conversion process, positively correlating the pyrolysis temperature used during production with the Cr immobilization efficiency of biochar ($r = 0.14$, $p < 0.05$, Table 5). When pyrolysis temperatures diverged from 300 to 500 °C and 501 to 700 °C, immobilization efficiency reached 46% and 63%, respectively. Biochar pH, which was affected by the temperature applied in production, also influenced the immobilization efficiency, which rose rapidly with higher pH ($r = 0.39$, $p < 0.05$) [55].

Soluble salts, contained in ash-rich biochars, increase the pH, enhancing its capacity for soil acidity and, therefore, decreasing the mobility of Cr in soil, while positively correlating the ash content ($r = 0.74$, $p < 0.01$) with the Cr immobilization efficiency for Cr [56].

There have been multiple studies linking the low effectiveness of unmodified biochar to scavenge Cr(VI), as a result of the low affinity of anionic pollutants to those adsorbents and the large Cr(VI) discharge into various types of ecosystems [57].

3.2. Biochar for Remediation of Cr Polluted Water

As indicated above, biochar's Cr(VI) removal performance directly depends on the production and modification parameters, pyrolysis temperature and pH of the solution. The most important factor in improving biochar's Cr(VI) sorption capacity is once again the pyrolysis temperature. Biochars produced under 300–400, 400–500, 500–600, 600–700 and 700–800 °C have average values of sorption capacities at 72.0, 69.1, 46.4, 43.7, and 99.2 mg/kg, respectively.

Pyrolysis temperature directly affects the amount of C(sp^3)-, C(sp^2)-, and O-containing functional groups (–C–O, CO and –COOH), which are the main factors controlling the electron-donating potential [58]. The mobility and the distribution of Cr(VI) is greatly influenced by the pH of the solution, as is the case for the mediation of the ionization of different-charged functional groups during sorption and reduction [59]. Typically, the Cr adsorption efficiency of biochars was exceptionally higher under low pH and reduced progressively by increasing pH to 8.

3.3. Modification of Biochar for Improved Cr Adsorption Efficiency

Functionalization of biochar rapidly increases the Cr(VI) sorption capacity of biochars [60].

3.3.1. Physical Activation of Biochars for Improving Cr Adsorption

Ball milling is a green, promising and low-cost technology which utilizes the dynamic energy of moving balls to practically grind biochar and provoke structural and chemical modifications. The technique can be performed either by physical means that modify the particle size and surface area, or by chemical means, which apart from the above, also modify the surface functional groups [61]. As a result, the surface of the material increases, its surface characteristics are boosted and its physiochemical properties are

modulated [62]. Naturally, the particle size of the biochar is influenced by both the treatment time and the rotational speed [63]. It is safe to conclude that the reduced particle size, the increased functionality, and the enlargement of the surface area, lead to an increased Cr immobilization capacity [64].

In a study by Zhu et al., 2019, the ball-milled biochar–Fe oxide composite showed a higher surface area (241 m^2/g), more abundant Fe oxides on the biochar surface, and mainly, a higher sorption capacity (48.1 mg/g) in comparison with the pristine biochar [65]. Likewise, ball-milling of a pyrite (FeS_2)-biochar composite increased its Cr(VI) sorption capacity to 134.0 mg/g, while also improving the homogeneity of the composite and reducing the agglomeration of the mineral.

UV irradiation modification, a method proposed as suitable for increasing the adsorption capacity for toxic elements, also seems to improve biochar functionality and multiply the Cr removal capacity compared with the pristine biochar, by as much as five times [66]. This particular method enhances the pore size distribution by greatly increasing the micropores. The most promising results, deriving from ball milling and UV irradiation methods, have the additional benefit of avoiding the use of chemical reagents.

Iced redox reactions of rice-husk-derived biochar have been attempted as a physical activation method for increasing Cr(VI) removal efficiency [67]. Freezing increased the accumulation of protons in the grain boundary, thus, enhancing the reduction of Cr(VI) and dissolving any organic matter.

Microwave pyrolysis generates microplasma spots that enhance the chemical reaction which activates biochar by increasing the local temperature. The mesopores' distribution on the surface increases, leading to enhanced Cr sorption. In comparison with conventional pyrolysis, microwave pyrolysis requires shorter time and lower temperature, to achieve the same yield, leading to lower energy consumption and a much lower cost. It is easily controlled with uniform temperature distributions, without needing pretreatments of the biomass used [68]. All of the above reasons elevate microwave pyrolysis to be among the most promising methods for biochar activation.

Steam/gas activation is another common method used in biochar modification, where the biochar is pyrolyzed with air, water vapor, and CO_2 at a specific temperature that varies between 650 and 950 °C. Superheated steam increases the formation of crystalline structures, generates surface oxides and hydrogen, when the carbon present on the surface of the biochar is exchanged with the oxygen of the water molecules [33], while also facilitating the formation of mesopores and micropores by clearing volatile compounds. The percentage of exchangeable cations is increased by the exposition of the biochar metal content [69]. Among the gases used, CO_2 increases the carbon content, when used in higher temperatures and longer reaction times. On the other hand, N_2 decomposes the amorphous substances more slowly, creating a less porous, acidic and polar biochar. No specific study has been conducted, but all of the above characteristics are believed to enhance the sorption of Cr on the material surface.

3.3.2. Sonication of Biochars for Improving Cr Adsorption

Sonication, a process that can be carried out either before or after pyrolysis, leads to advanced leaching of the minerals contained in biochars (such as Na, K, Fe, Al), which causes swelling and improvement of the internal surface area. In this way, modification of the biochar properties is achieved externally and internally, rapidly increasing the adsorption capacity of the material [60]. Further characterization shows an increase in the material mesopores, which naturally increase the physicochemical and adsorption properties of the biochar. When it comes to Cr, the increased microporosity enhances the retention of the metal.

3.3.3. Chemical Modification of Biochars for Improving Cr Adsorption

Biochar Magnetization

Biochar magnetization by grafting ferromagnetic materials (e.g., Fe, Co, Ni and their alloys) into the carbonaceous matrix of biochar, leads to exceptional post sorption separation by using an external magnetic field. Qipao et al. synthesized a mixture of *Enteromorpha prolifera* biochar/Fe powder/hollow glass microspheres which were added to a sodium alginate solution, thus, creating a magnetized Cr(VI) adsorbent [70]. The material achieved Cr(VI) removal of 87.7% with potential for extra removal after three regeneration cycles.

Fe-modification, either pre- or post-pyrolysis, also gives exceptional results. The Fe premodification biochars, in particular, appear to be more magnetized and more acidic, resulting in higher Cr(VI) attraction.

There are strong indications that the existence of electron donors on the surfaces of different magnetic biochars leads to the reduction of Cr(VI) to Cr(III), which can be divided using an external magnetic field. Current studies have focused on the optimum modification conditions for achieving the highest adsorption capacity and reusability. Amongst all the Fe-based modifications, impregnation of biochar in ferric chloride solutions has exhibited the highest Cr(VI) removal percentages compared with modification with citric acid, and sodium hydroxide [71]. For example, an $FeCl_3$ impregnated magnetic Lantana camara biochar exhibited high Cr(VI) sorption capacity (102.0 mg/g). Pre-pyrolysis modification with magnetic particles on biochar surfaces produced greater surface areas, while post-pyrolysis modification increased protonated O-rich groups such as CO and –OH located on the biochar surface. N-doped magnetic biochar also showed a high Cr(VI) sorption capacity (142.9 mg/g), while also being easy to separate from the medium [72].

To conclude, high Cr removal is achieved from aquatic solutions by magnetic biochars, with improved reusability. In addition, further research is needed to study the potential of reusing the magnetic biochars, with an aim to increase their efficiency and lifespan.

Biochar Supported Reductant Materials

One of the most common biochar modifications is the use of reductant materials such as iron and sulfur composites supported on the biochar surface. Although the principles of the methods differ, the Fe-biochars produced appear to have lesser or equal magnetic properties to that of the magnetic biochars. Through this method, materials with great Cr(VI) reduction capacity in both soil and wastewater are obtained, whereas biochar magnetization focuses on creating materials easily separated after their use. Antoniadis et al., (2017) synthesized a nZVI-biochar–chitosan composite exhibiting a much higher Cr(VI) sorption capacity than pristine biochars [73]. In addition, the nZVI-doped biochar showed high reducing potential, which resulted in near-complete removal of Cr(VI) from the contaminated area. Fe (II) donates electrons through the biochar–Fe–Cr electron transfer route and becomes oxidized to Fe (III) while doing so. It is clear that iron species play an important role in the reduction of Cr(VI). Multiple minerals have been used to modify biochar and reduce Cr(VI) to Cr(III) such as pyrite (FeS_2) and mackinawite (FeS) [74]:

$$Cr^{6+}{}_{(aq)} + 3Fe^{2+}{}_{(aq)} \rightarrow Cr^{3+} + 3Fe^{3+}$$

Mackinawite, in particular, is a mineral with high Cr(VI) immobilization when supported on biochar, because in that way agglomeration of the FeS particles is avoided [74]. In addition to metal-based modification techniques, Cr(VI) reduction can be achieved by maintaining acidic conditions during treatment. Dong et al., (2011) used sugar beet tailing biochar, with Cr(III) being reduced through electrostatic interaction between negatively-charged Cr(VI) ions and cationic biochar [75].

In conclusion, reducing agents play a major role in Cr(VI) elimination, as they can enhance the reduction process and expedite adsorption of Cr onto the biochar surfaces.

The method produces biochar with high Cr adsorption efficiency, making it ideal for Cr remediation.

Enrichment of Active Functional Groups on Biochar Surfaces

The functional groups on the surface of the biochar have a very important role in the decontamination of Cr. Several studies have achieved chemical activation of the biochar by increasing the abundance of functional groups on the biochar surface, that include CO, –OH and $–NH_2$. Chakraborty and Das used polyethylenimine to enrich the biochar surface with amino groups, improving the adsorption capacity for Cr(VI) by up to 10-fold in comparison with pristine biochar [76]. In general, impregnation of minerals has been used to introduce amino groups onto biochar surfaces for improved functionality. Apart from that, biochar polymerization with various polymers, such as acrylamide, increased the percentage of multiple functional groups (e.g., –CO, –C–O and C–N). Chitosan–biochar composites, whose surfaces were loaded with amino and hydroxyl groups, showed a four-fold increased sorption capacity for Cr. O-containing surface functional groups (e.g., –OH, –COOH and –C–O) might significantly contribute to the reduction of Cr(VI) to Cr(III) in contaminated soils, since they serve as proton donors.

Nanocomposites of Biochar Matrix

Nanocomposites of biochar matrix have been used for immobilizing Cr(VI), combining the potential of both components to immobilize heavy metals. Nano-magnetite and siltstone composite supported on biochar showed a higher sorption capacity than the unmodified biochar (35.6 mg/g vs. 26.2 mg/g). In addition, siltstone greatly improved the stability of the composite during the thermochemical conversion process [77]. Intensive functional groups and higher surface area led to an increase in the Cr(VI) adsorption capacity of the biochar–nano-composites materials. Therefore, despite the need for further investigation of the potentially available mechanisms, this method is very promising.

Heteroatom Dopants Incorporation

Heteroatom dopant incorporation led to an electron-withdrawing effect, which raised the percentage of positive charges for effective binding of electronegative contaminants such as Cr(VI). Of all the different heteroatom dopants, transition metal nanoparticles displayed exceptionally good catalysis capacity for the reduction of Cr(VI) [78]. Utilizing nitrogen or/and oxygen as heteroatom dopants also increased the active functional groups leading to an improvement in the functionality of biochar [79]. A large surface area (1525 m^2/g) and exceptionally high Cr(VI) sorption capacity (217.4–312.5 mg/g) were obtained when N and S were incorporated in biochar-like carbon sheets [80]. Shrimp shell magnetic biochar incorporated with N-doped graphene oxide 3-D hydrogel was used to eliminate Cr(VI) from aquatic environments. The decorated nanocomposite had a higher surface area than the magnetic shrimp shell biochar, and a higher sorption capacity, as a result of electrostatic attraction and reduction, with the total elimination of Cr(VI) fluctuating between 98.0 and 99.8% [81].

Acid and Alkali Treatment of Biochars

Undeniably, the most common modifications of biochars are acid and alkali treatments. These methods rapidly enhance the reduction of the metal and, consequently, the sorption of Cr(III). Acid and alkali treatments increase the availability of electrons that originate from compounds already existing in the matrix of biochar such as anhydrous sugars, catechol, and diols. Evaluation of the effect of acid (0.5 mol/L H_2SO_4) or alkali (0.5 mol/L NaOH) treatments on biochar removal capacity of heavy metals and functionality by Xiao et al., 2015, showed that alkali treatment increased the point zero charge and enriched the material with functional aromatic CO– and phenolic –OH groups [82]. On the other hand, acidic treatment reduced the biochar ash content and protonated the O-containing groups [83]. Acid-treated biochar had a significantly higher removal capacity than the

alkali-treated biochar (89.9 vs. 53.5%). Dianat Maharlouei et al. studied the effect of acidic (H_2SO_4, and HNO_3) and alkalic (KOH and NaOH) modification of rice husk and almond (*Prunus dulcis* L.) soft husk biochars on the removal of Cr from soil [84]. The modified biochars showed the highest reduction capacity for Cr(VI), while the NaOH-treated rice husk biochar had the lowest removal efficiency for Cr.

In another study, different types of mangosteen shells were used as biomass to synthesize biochar (Z2PT350-700) [85]. HCl, KOH and $ZnCl_2$ were used to modify the biochar, while applying different pyrolysis conditions and processes. Z2PT350-700 exhibited great Cr(VI) removal efficiency in aquatic environments, as a result of its physical and chemical characteristics that allowed surface complexation, electrostatic interaction, and ion exchange.

To conclude, acidic modification increased biochar surface area, functional groups, and surface hydrophilicity, while alkali modification increased porous structure and surface phenolic and –OH groups. Both techniques succeeded in producing biochar with exceptional Cr removal efficiency, while it is also possible to use them synergistically with other techniques. Table 6 lists various ways of synthesizing and modifying biochars, as well as interesting results of each method.

Table 6. Biochars by different types of biomasses and their characteristics (PT: pyrolysis temperature; PS: pore size; SA: surface area; TPV: total pore volume).

Biomass	Production Condition	Modification Type	Pollutant	Maximum Removal	Points Of Interest	Author
Waste mangosteen shells	PT = 350, 700 °C; duration = 0.5 h, 1.5 h; SA = 1.64–1836.46 m^2/g; TPV = 0.004–1.058 cm^3/g	HCl, KOH and $ZnCl_2$	Cr(VI)	212.6 mg/g at pH 2	The physical/chemical characteristics of the tailored biochar was imitated by the electrostatic interaction, surface complexation, and ion exchange in the elimination of Cr(VI).	[85]
Apple wood	PT = 700 °C; SA = 0.0921 m^2/g; TPV = 0.00108 cm^3/g; PS = 1.0487 nm	–	Cr(VI)	0.10–7.71 mg/g at pH 2	The electrostatic attraction, Cr(VI) reduction, Cr(III) complexation, and ion exchange were possible mechanisms involved in Cr(VI) removal.	[86]
Beet tailing	PT = 300 °C; duration = 2 h; SA = 137 m^2/g	-	Cr(VI)	123 mg/g at pH 2	Cr(VI) removal mechanisms included electrostatic attraction, reduction and complexation.	[75]
Shrimp shell	SA = 398.1 m^2/g	Heteroatom decoration	Cr(VI)	350.42 mg/g	N_2 active contribution in electrostatic attraction, pore filling and reduction mechanisms.	[81]
Farmyard and poultry manure	PT = 450 °C; duration = 3 h; SA = 9.01, 10.23 m^2/g; ash = 31.51, 27.21%	–	Cr(III)	37.75 and 33.94 mg/g	Removal of Cr(III) was achieved through chemisorption.	[87]
Tobacco petiole	PT = 300–700 °C; duration = 0.5 h SA = 0.42–7.51 m^2/g; ash = 11.6%	–	Cr(VI) and Cr_{total}	66.7% (Cr(VI)) and 21.1% (Cr_{total}) at pH 1.	Increase in pyrolytic temperature reduced Cr(VI) adsorption efficiency.	[88]
Plum and apricot kernels	PT = 500 °C; duration = 1 h; SA = 146.6, 85.6 m^2/g; TPV = 0.09, 0.14 cm^3/g; PS = 12.23, 32.85 Å ash = 0.81, 1.12%	–	Cr(III)	>70% at pH 6 and 7	High adsorption efficiency because of the surface complexation of surface functional groups (S-containing functional groups).	[89]
Corn cobs	Hydrothermal treatment temperature = 300 °C; duration = 0.5 h	Polyethylene imine (PEI)	Cr(VI)	33.663 mg/g	Improvement of adsorption of Cr(VI) up to 365%, compared with unmodified hydrochar.	[90]
Corn straw	PT = 300, 500, 700 °C; duration = 2 h; SA = 5.09, 241.83, 417.83 m^2/g; TPV = 0.0036, 0.1472, 0.2391 cm^3/g; PS = 35.16, 3.76, 4.63 nm; ash = 0.44, 1.70, 2.56%	HNO_3 activation	Cr(VI)	33.33 mg/g at pH∼7	EPFRs on biochars played a key role in reduction of Cr(VI) at neutral pH.	[91]

Table 6. *Cont.*

Biomass	Production Condition	Modification Type	Pollutant	Maximum Removal	Points Of Interest	Author
Blooms of Enteromorpha prolifera	PT = 500 °C	Biochar magnetization	Cr(III), Cr(VI)	18.24 mg/g, 11.13 mg/g	The beads could selectively adsorb chromium while their magnetic properties allowed them to be easily reclaimable.	[70]
Rice husk	PT = 775 °C	Polyethylenimine	Cr(VI)	435.7 mg/g at pH 2	Modification significantly improved the adsorption performance for Cr(VI) removal.	[66]
Willow residue	PT = 700 °C; duration = 2 h; SA = 100.6095 m^2/g	Ball milling, nanoscale zero valent iron modification	Cr(VI)	500 mg k/g at pH 6.14	The increase in Cr(VI) removal by amendments contributed to the increase in the migration of NO_3-–N from roots to shoots.	[65]
Switch grass	PT = 425, 700 °C; duration = 60 s SA = 1.1 m^2/g ash = 13.92%	KOH, by *Zhihengliuella* sp. *ISTPL4*	Cr(VI)	100%	Immobilized enzyme showed maximum adsorption efficiency.	[92]

3.3.4. Activation of Biochars by Microorganisms and Their Metabolites

Biological activation includes modification using organisms and their metabolites and is an eco-friendly method. This technique can achieve outstanding removal capacity because of the effect of biochar on Cr(VI) toxicity on microbial activities. Mishra et al. investigated the potential for the production of biochar by *Zhihengliuella* sp. *ISTPL4* to effectively remove Cr(VI) from aqueous solutions [92]. The composite showed exceptional removal capacity of 100%, corresponding to 87.7% immobilization, and 12.3% to the residual non-toxic Cr(III) in the solution. Matern and Mansfeldt also studied the reduction of Cr(VI) by Fe(II)-biochar composite [93]. Through a reduction process, iron–Cr co-precipitates were synthesized. The biogenic Fe(II)-biochar composite had a higher removal efficiency by 30%, in comparison with Fe minerals. It is safe to conclude that a combination of microorganisms and organic microsorbents is especially effective in removing Cr(VI), and can provide practical and environmentally friendly techniques for decontamination.

3.4. Mechanisms of Cr Adsorption

Cr(VI) elimination can follow multiple different routes, such as reduction of hexavalent chromium to trivalent chromium and adsorption (physical and/or chemical) on the surface of biochars. Amongst the above, electrostatic attraction is one of the most common Cr immobilization mechanisms, a result of the negative charge of the biochar surface functional groups that attract the positively charged chromium ions. Variable negative charges on biochar surface build the high electronegativity of the material. Those charges derive from specific functional groups which increase with the pH. This is the reason why Cr sorption onto biochar surface is pH-dependent, along with the fact that Cr speciation changes with pH. For instance, the Cr (100 mg/L) at pH 3.0 in an aqueous solution is composed of Cr^{3+} (87%), $CrOH^{2+}$ (11%) and $Cr_2(OH)_2{}^{4+}$ (2%); however, increasing pH to 4.0 changes speciation to Cr^{3+} (30%), $CrOH^{2+}$ (40%), Cr_2 $(OH)_2{}^{4+}$ (26%) and $Cr_3(OH)_4{}^{5+}$ (4%) [94].

When it comes to biochar, when the solution pH is higher than the pH_{zpc}, its surface becomes negatively charged, increasing the material affinity with positively charged ions. When the solution pH is lower than the $pH_{zpc,}$ the protonation of the biochar surface charges it, positively increasing the material affinity with negatively charged ions [81].

Choppala et al., 2018, reported that Cr(III) electrostatic attraction by rice, peanut, canola and soybean straws was marginal in acidic conditions, as a result of the abundance of H^+ ions and the positively charged biochar surfaces [11].

Adsorption of Cr starts with the reduction of Cr(VI) to Cr(III). The pH regulates the reduction efficiency of biochar as it affects the surface functional groups including acidic (e.g., –COOH, C–O and CO) and basic (e.g., chromone, ketone and pyrone) groups [95], that can act as electron donors reducing Cr(VI) to Cr(III). This transfer of electrons via π-π electron donor–acceptor interaction is enhanced by the conductive carbon regions present on biochar surface and is followed by the adsorption of Cr [96]. The release of dissolved

organic matter from the biochar also contributes to the reduction of the metal [11] along with the high porous polycyclic aromatic hydrocarbon sheets [75].

Surface functional groups participate more actively in the immobilization of Cr than interior functional groups [97]. The functional groups that greatly affect biochar efficiency depend on the biomass used as feedstock as well as the conditions of the biochar production.

In the reaction of Cr(VI) with peanut shell biochar, there is a large reduction in the abundance of –C–O groups and an increase in the proportion of –COO– and –CO groups, indicating that –C–O groups act as electron-donating areas, reducing Cr(VI) and being oxidized into –COO– and –CO groups [36]. Apart from that, protonated OH^+ and $–NH_2^+$ groups also actively participate in Cr(VI) removal [98].

This electron donation can be described as [99]:

$$HCrO^{7-} + 7H^+ + 3e^- \leftrightarrow 4H_2O \text{ (Eo = +1.35)}.$$

The FTIR analysis of the biochar after adsorption, confirmed the –OH and –COOH groups' participation in Cr complexation, where beneficial changes in the peak intensities of oxygen containing functional groups were observed [100].

The possible mechanisms for Cr removal are cation and anion exchange with Cr(III) and Cr(VI). The X-ray absorption near-edge structure and extended X-ray absorption fine structure techniques indicated that the mechanisms followed by oak wood biochar for the removal of Cr(VI) were firstly electrostatic attraction, then reduction to Cr(III) and diffusion on the inner surfaces, and finally Cr(III) desorption by ion exchange [101]. Anion exchange with Cl^- contribution in Cr(VI) sorption was about 36% in a magnetic corncob composite consisting of biochar and polypyrrole [102].

Another widely studied mechanism for chromium immobilization is (co)precipitation. In a study by He et al., oak wood biochar—ZVI nanocomposite—removed 100% of Cr(VI) via multiple mechanisms that included all of the above methods (electrostatic attraction, diffusion, etc.) [103]. The un-adsorbed Cr(III) ions co-precipitated as combined Cr(III)/Fe(III) hydroxides.

Last but not least, physical adsorption of Cr into the biochar pores is a necessary final step for the removal of Cr from the environment, however the specific mechanisms followed are unclear and in need of further investigation.

3.5. Biochar Regeneration

One of the most important abilities of any potential adsorbent for practical use is its ability to be regenerated and reused, an ability that rapidly reduces the overall technology cost. In any synthesis, it is crucial to evaluate the reusability and regeneration capacity of the material. The most common regeneration method is acid or alkali wash, although many techniques are being employed. Through the process, the adsorption sites become available for further elimination cycles. Several approaches have been utilized to this end, such as magnetic separation, centrifugation, filtration, etc. [104]. Naturally, there is loss in the adsorption efficiency over successive cycles as a result of the loss of surface-active sites or/and functional groups. The adsorbents that are unfit for reuse are usually carefully disposed through landfilling and incineration [105]. In that way, the financial and environmental cost of the process is kept as low as possible.

4. Conclusions

Environmental pollution by arsenic (As) and hexavalent chromium (Cr(VI)) has been one of the most serious environmental problems in recent years. Arsenic adsorption using sorbents based on biochar was summarized as an effective and financially viable method. The aim of this review was to provide a recent literature overview of the different biochar modification methods, as well as of the factors that influence their capacity to successfully remove As and Cr(VI).

The pyrolytic temperature, residence duration, feedstock, and pyrolysis technology all have an impact on the characteristics of arsenic adsorption. The ability to remove As(III) as

well as As(V) is significantly improved by modified biochar adsorbents (with cationic character), due to their high porosity and reactivity, after surface modification. Arsenic remediation by rice husk biochar has produced highly promising results, and more importantly, demonstrated that condition adjustments and modification can optimize remediation.

Regarding the removal of chromium, there is a direct relationship between the environmental condition and the removal rate, as these conditions determine the oxidation state of the pollutant. In order to achieve maximum removal, it is necessary to properly modify plain biochar, using a variety of methods, each of which has its own advantages and disadvantages. Finally, the biomass used also affects the removal capacity, as it determines the biochars' surface functional groups.

Author Contributions: Conceptualization, A.K.T. and I.A.K.; methodology, S.C., M.X., A.K.T. and I.A.K.; validation, A.K.T. and I.A.K.; formal analysis, S.C., M.X., A.K.T. and I.A.K.; investigation, S.C., M.X., A.K.T. and I.A.K.; resources, S.C., M.X., A.K.T. and I.A.K.; data curation, S.C., M.X. and A.K.T.; writing—original draft preparation, S.C., M.X. and A.K.T.; writing—review and editing, S.C., M.X. and A.K.T.; supervision, A.K.T. and I.A.K. All authors have read and agreed to the published version of the manuscript.

Funding: This research received no external funding.

Institutional Review Board Statement: Not applicable.

Informed Consent Statement: Not applicable.

Data Availability Statement: All data analyzed during this study are included in this published article.

Conflicts of Interest: The authors declare no conflict of interest.

References

1. Rasool, A.; Xiao, T.; Farooqi, A.; Shafeeque, M.; Liu, Y.; Kamran, M.A.; Katsoyiannis, I.A.; Eqani, S.A.M.A.S. Quality of tube well water intended for irrigation and human consumption with special emphasis on arsenic contamination at the area of Punjab, Pakistan. *Environ. Geochem. Health* **2017**, *39*, 847–863. [CrossRef] [PubMed]
2. Katsoyiannis, I.A.; Mitrakas, M.; Zouboulis, A. Arsenic occurrence in Europe: Emphasis in Greece and description of the applied full-scale treatment plants. *Desalination Water Treat.* **2015**, *54*, 2100–2107. [CrossRef]
3. Kaprara, E.; Kazakis, N.; Simeonidis, K.; Coles, S.; Zouboulis, A.; Samaras, P.; Mitrakas, M. Occurrence of Cr(VI) in drinking water of Greece and relation to the geological background. *J. Hazard. Mater.* **2015**, *281*, 2–11. [CrossRef] [PubMed]
4. Tumolo, M.; Ancona, V.; De Paola, D.; Losacco, D.; Campanale, C.; Massarelli, C.; Uricchio, V.F. Chromium Pollution in European Water, Sources, Health Risk, and Remediation Strategies: An Overview. *Int. J. Environ. Res. Public Health* **2020**, *17*, 5438. [CrossRef] [PubMed]
5. Laskaridis, A.; Sarakatsianos, I.; Tzollas, N.; Katsoyiannis, I. Simultaneous Removal of Arsenate and Chromate from Ground- and Surface- Waters by Iron-Based Redox Assisted Coagulation. *Sustainability* **2020**, *12*, 5394. [CrossRef]
6. Flora, S.J.S. *Handbook of Arsenic Toxicology*; Academic Press: Oxford, UK, 2015; pp. 1–49.
7. ATSDR. *Agency for Toxic Substances and Disease Registry Justification of Appropriation Estimates for Appropriations Committees Fiscal Year 2021*; Agency for Toxic Substances and Disease Registry (ATSDR), Department of Health and Human Services: Atlanta, GA, USA, 2020. Available online: https://stacks.cdc.gov/view/cdc/109265 (accessed on 6 November 2022).
8. Podgorski, J.; Berg, M. Global threat of arsenic in groundwater. *Science* **2020**, *368*, 845–850. [CrossRef] [PubMed]
9. The Council of the European Union. *Council Directive 98/83/on EC of 3 November 1998 the Quality of Water Intended for Human Consumption*; Cambridge University Press: Cambridge, UK, 2010; pp. 32–54.
10. Pal, P. Groundwater Arsenic Remediation: Treatment Technology and Scale Up. Elsevier: Oxford, UK, 2015.
11. Choppala, G.; Kunhikrishnan, A.; Seshadri, B.; Park, J.H.; Bush, R.; Bolan, N. Comparative sorption of chromium species as influenced by pH, surface charge and organic matter content in contaminated soils. *J. Geochem. Explor.* **2018**, *184*, 255–260. [CrossRef]
12. Enya, O.; Lin, C.; Qin, J. Heavy metal contamination status in soil-plant system in the Upper Mersey Estuarine Floodplain, Northwest England. *Mar. Pollut. Bull.* **2019**, *146*, 292–304. [CrossRef]
13. EPA, U. Chromium compounds: Hazard summary. *Natl. Cent. Environ. Assess.* **1973**, 639–700.
14. WHO. World Health Organization European Standards for Drinking-Water. *Am. J. Med. Sci.* **1970**, *242*, 56.
15. Kumar, R.; Patel, M.; Singh, P.; Bundschuh, J.; Pittman, C.U., Jr.; Trakal, L.; Mohan, D. Emerging technologies for arsenic removal from drinking water in rural and peri-urban areas: Methods, experience from, and options for Latin America. *Sci. Total Environ.* **2019**, *694*, 133427. [CrossRef]

16. Baskan, M.B.; Pala, A. Removal of arsenic from drinking water using modified natural zeolite. *Desalination* **2011**, *281*, 396–403. [CrossRef]
17. Losev, V.N.; Didukh-Shadrina, S.L.; Orobyeva, A.S.; Metelitsa, S.I.; Borodina, E.V.; Ondar, U.V.; Nesterenko, P.N.; Maznyak, N.V. A new method for highly efficient separation and determination of arsenic species in natural water using silica modified with polyamines. *Anal. Chim. Acta* **2021**, *1178*, 338824. [CrossRef]
18. Jacobson, A.T.; Fan, M. Evaluation of natural goethite on the removal of arsenate and selenite from water. *J. Environ. Sci.* **2019**, *76*, 133–141. [CrossRef]
19. Sø, H.U.; Postma, D.; Jakobsen, R.; Larsen, F. Sorption and desorption of arsenate and arsenite on calcite. *Geochim. Et Cosmochim. Acta* **2008**, *72*, 5871–5884. [CrossRef]
20. Zhu, H.; Jia, Y.; Wu, X.; Wang, H. Removal of arsenic from water by supported nano zero-valent iron on activated carbon. *J. Hazard. Mater.* **2009**, *172*, 1591–1596. [CrossRef] [PubMed]
21. Yao, S.; Liu, Z.; Shi, Z. Arsenic removal from aqueous solutions by adsorption onto iron oxide/activated carbon magnetic composite. *J. Environ. Health Sci. Eng.* **2014**, *12*, 58. [CrossRef] [PubMed]
22. Shakoor, M.B.; Niazi, N.K.; Bibi, I.; Murtaza, G.; Kunhikrishnan, A.; Seshadri, B.; Shahid, M.; Ali, S.; Bolan, N.S.; Ok, Y.S.; et al. Remediation of arsenic-contaminated water using agricultural wastes as biosorbents. *Crit. Rev. Environ. Sci. Technol.* **2016**, *46*, 467–499. [CrossRef]
23. Liu, Z.; Xu, Z.; Xu, L.; Buyong, F.; Chay, T.C.; Li, Z.; Cai, Y.; Hu, B.; Zhu, Y.; Wang, X. Modified biochar: Synthesis and mechanism for removal of environmental heavy metals. *Carbon Res.* **2022**, *1*, 8. [CrossRef]
24. Andjelkovic, I.; Jovic, B.; Jovic, M.; Markovic, M.; Stankovic, D.; Manojlovic, D.; Roglic, G. Microwave-hydrothermal method for the synthesis of composite materials for removal of arsenic from water. *Environ. Sci. Pollut. Res.* **2015**, *23*, 469–476. [CrossRef]
25. Khan, S.A.; Imteaz, M.A. Batch experiments on arsenic removal efficiencies through adsorption using synthetic and natural sand samples. *Int. J. Environ. Sci. Technol.* **2021**, *18*, 2357–2364. [CrossRef]
26. Tolkou, A.K.; Katsoyiannis, I.A.; Zouboulis, A.I. Removal of Arsenic, Chromium and Uranium from Water Sources by Novel Nanostructured Materials Including Graphene-Based Modified Adsorbents: A Mini Review of Recent Developments. *Appl. Sci.* **2020**, *10*, 3241. [CrossRef]
27. Tolkou, A.K.; Kyzas, G.Z.; Katsoyiannis, I.A. Arsenic(III) and Arsenic(V) Removal from Water Sources by Molecularly Imprinted Polymers (MIPs): A Mini Review of Recent Developments. *Sustainability* **2022**, *14*, 5222. [CrossRef]
28. Koutzaris, S.; Xanthopoulou, M.; Laskaridis, A.; Katsoyiannis, I.A. H_2O_2-Enhanced As(III) Removal from Natural Waters by Fe(III) Coagulation at Neutral pH Values and Comparison with the Conventional Fe(II)-H_2O_2 Fenton Process. *Sustainability* **2022**, *14*, 16306. [CrossRef]
29. Bolan, N.; Hoang, S.A.; Beiyuan, J.; Gupta, S.; Hou, D.; Karakoti, A.; Joseph, S.; Jung, S.; Kim, K.-H.; Kirkham, M.; et al. Multifunctional applications of biochar beyond carbon storage. *Int. Mater. Rev.* **2022**, *67*, 150–200. [CrossRef]
30. Jobby, R.; Jha, P.; Yadav, A.K.; Desai, N. Biosorption and biotransformation of hexavalent chromium [Cr(VI)]: A comprehensive review. *Chemosphere* **2018**, *207*, 255–266. [CrossRef]
31. Tolkou, A.K.; Trikalioti, S.; Makrogianni, O.; Xanthopoulou, M.; Deliyanni, E.A.; Katsoyiannis, I.A.; Kyzas, G.Z. Chromium(VI) Removal from Water by Lanthanum Hybrid Modified Activated Carbon Produced from Coconut Shells. *Nanomaterials* **2022**, *12*, 1067. [CrossRef]
32. Tolkou, A.K.; Vaclavikova, M.; Gallios, G.P. Impregnated Activated Carbons with Binary Oxides of Iron-Manganese for Efficient Cr(VI) Removal from Water. *Water Air Soil Pollut.* **2022**, *233*, 343. [CrossRef]
33. Li, Y.; Xing, B.; Ding, Y.; Han, X.; Wang, S. A critical review of the production and advanced utilization of biochar via selective pyrolysis of lignocellulosic biomass. *Bioresour. Technol.* **2020**, *312*, 123614. [CrossRef]
34. Zhang, Y.; Zhang, J.; Song, K.; Lv, W. Potential of biochar derived from three biomass wastes as an electrode catalyzing oxygen reduction reaction. Environ. *Pollut. Bioavailab.* **2022**, *34*, 42–50. [CrossRef]
35. Lehmann, J.; Joseph, S. *Biochar for environmental management: An introduction. Biochar for Environmental Management: Science, Technology and Implementation*; Routledge: London, UK, 2015. [CrossRef]
36. Rajapaksha, A.U.; Alam, S.; Chen, N.; Alessi, D.S.; Igalavithana, A.D.; Tsang, D.C.; Ok, Y.S. Removal of hexavalent chromium in aqueous solutions using biochar: Chemical and spectroscopic investigations. *Sci. Total Environ.* **2018**, *625*, 1567–1573. [CrossRef] [PubMed]
37. Liu, H.; Li, P.; Qiu, F.; Zhang, T.; Xu, J. The Application of Eco-Friendly Fe-Al Bimetallic Oxide/Biochar Adsorbent Composites with Waste Rice Husk for Removal of Arsenic at Low Concentration. *J. Inorg. Organomet. Polym. Mater.* **2022**, *32*, 122–133. [CrossRef]
38. Lee, J.; Sarmah, A.K.; Kwon, E.E. Production and Formation of Biochar. In *Biochar from Biomass and Waste*; Ok, Y.S., Tsang, D.C.W., Bolan, N., Novak, J.M., Eds.; Elsevier: Amsterdam, The Netherlands, 2019; pp. 3–18. [CrossRef]
39. Vithanage, M.; Herath, I.; Joseph, S.; Bundschuh, J.; Bolan, N.; Ok, Y.S.; Kirkham, M.; Rinklebe, J. Interaction of arsenic with biochar in soil and water: A critical review. *Carbon* **2017**, *113*, 219–230. [CrossRef]
40. Mohan, D.; Pittman, C.U., Jr. Arsenic removal from water/wastewater using adsorbents—A critical review. *J. Hazard. Mater.* **2007**, *142*, 1–53. [CrossRef]
41. Zhang, W.; Lin, N.; Liu, D.; Xu, J.; Sha, J.; Yin, J.; Tan, X.; Yang, H.; Lu, H.; Lin, H. Direct carbonization of rice husk to prepare porous carbon for supercapacitor applications. *Energy* **2017**, *128*, 618–625. [CrossRef]

42. Shinogi, Y.; Kanri, Y. Pyrolysis of plant, animal and human waste; physical and chemical characterization of pyrolytic products. *Bioresour. Technol.* **2003**, *90*, 241–247. [CrossRef]
43. Samsuri, A.W.; Sadegh-Zadeh, F.; Seh-Bardan, B.J. Adsorption of As(III) and As(V) by Fe coated biochars and biochars produced from empty fruit bunch and rice husk. *J. Environ. Chem. Eng.* **2013**, *1*, 981–988. [CrossRef]
44. Abu Sari, N.; Ishak, C.F.; Abu Bakar, R. Characterization of Oil Palm Empty Fruit Bunch and Rice Husk Biochars and Their Potential to Adsorb Arsenic and Cadmium. *Am. J. Agric. Biol. Sci.* **2014**, *9*, 450–456. [CrossRef]
45. Agrafioti, E.; Kalderis, D.; Diamadopoulos, E. Arsenic and chromium removal from water using biochars derived from rice husk, organic solid wastes and sewage sludge. *J. Environ. Manag.* **2014**, *133*, 309–314. [CrossRef]
46. Agrafioti, E.; Kalderis, D.; Diamadopoulos, E. Ca and Fe modified biochars as adsorbents of arsenic and chromium in aqueous solutions. *J. Environ. Manag.* **2014**, *146*, 444–450. [CrossRef]
47. Pan, J.-J.; Jiang, J.; Qian, W.; Xu, R.-K. Arsenate Adsorption from Aqueous Solution onto Fe(III)-Modified Crop Straw Biochars. *Environ. Eng. Sci.* **2015**, *32*, 922–929. [CrossRef]
48. Wu, C.; Huang, L.; Xue, S.-G.; Huang, Y.-Y.; Hartley, W.; Cui, M.-Q.; Wong, M.-H. Arsenic sorption by red mud-modified biochar produced from rice straw. *Environ. Sci. Pollut. Res.* **2017**, *24*, 18168–18178. [CrossRef] [PubMed]
49. Priyadarshni, N.; Nath, P.; Nagahanumaiah; Chanda, N. Sustainable removal of arsenate, arsenite and bacterial contamination from water using biochar stabilized iron and copper oxide nanoparticles and associated mechanism of the remediation process. *J. Water Process Eng.* **2020**, *37*, 101495. [CrossRef]
50. Shen, Z.; Jin, J.; Fu, J.; Yang, M.; Li, F. Anchoring Al- and/or Mg-oxides to magnetic biochars for Co-uptake of arsenate and fluoride from water. *J. Environ. Manag.* **2021**, *293*, 112898. [CrossRef] [PubMed]
51. Cuong, D.V.; Wu, P.-C.; Chen, L.-I.; Hou, C.-H. Active MnO_2/biochar composite for efficient As(III) removal: Insight into the mechanisms of redox transformation and adsorption. *Water Res.* **2021**, *188*, 116495. [CrossRef] [PubMed]
52. Benis, K.Z.; Damuchali, A.M.; Soltan, J.; McPhedran, K.N. Treatment of aqueous arsenic—A review of biochar modification methods. *Sci. Total Environ.* **2020**, *739*, 139750. [CrossRef] [PubMed]
53. Zhang, W.; Cho, Y.; Vithanage, M.; Shaheen, S.M.; Rinklebe, J.; Alessi, D.S.; Hou, C.-H.; Hashimoto, Y.; Withana, P.A.; Ok, Y.S. Arsenic removal from water and soils using pristine and modified biochars. *Biochar* **2022**, *4*, 55. [CrossRef]
54. Jian, X.; Li, S.; Feng, Y.; Chen, X.; Kuang, R.; Li, B.; Sun, Y. Influence of Synthesis Methods on the High-Efficiency Removal of Cr(VI) from Aqueous Solution by Fe-Modified Magnetic Biochars. *ACS Omega* **2020**, *5*, 31234–31243. [CrossRef]
55. An, Q.; Li, X.-Q.; Nan, H.-Y.; Yu, Y.; Jiang, J.-N. The potential adsorption mechanism of the biochars with different modification processes to Cr(VI). *Environ. Sci. Pollut. Res.* **2018**, *25*, 31346–31357. [CrossRef]
56. El-Naggar, A.; Lee, M.-H.; Hur, J.; Lee, Y.H.; Igalavithana, A.D.; Shaheen, S.M.; Ryu, C.; Rinklebe, J.; Tsang, D.C.; Ok, Y.S. Biochar-induced metal immobilization and soil biogeochemical process: An integrated mechanistic approach. *Sci. Total Environ.* **2020**, *698*, 134112. [CrossRef]
57. Deng, Y.; Huang, S.; Laird, D.A.; Wang, X.; Meng, Z. Adsorption behaviour and mechanisms of cadmium and nickel on rice straw biochars in single- and binary-metal systems. *Chemosphere* **2019**, *218*, 308–318. [CrossRef] [PubMed]
58. Chen, X.-L.; Li, F.; Xie, X.J.; Li, Z.; Chen, L. Nanoscale Zero-Valent Iron and Chitosan Functionalized *Eichhornia crassipes* Biochar for Efficient Hexavalent Chromium Removal. *Int. J. Environ. Res. Public Health* **2019**, *16*, 3046. [CrossRef] [PubMed]
59. Mandal, S.; Sarkar, B.; Bolan, N.; Ok, Y.S.; Naidu, R. Enhancement of chromate reduction in soils by surface modified biochar. *J. Environ. Manag.* **2017**, *186*, 277–284. [CrossRef] [PubMed]
60. Ambika, S.; Kumar, M.; Pisharody, L.; Malhotra, M.; Kumar, G.; Sreedharan, V.; Singh, L.; Nidheesh, P.; Bhatnagar, A. Modified biochar as a green adsorbent for removal of hexavalent chromium from various environmental matrices: Mechanisms, methods, and prospects. *Chem. Eng. J.* **2022**, *439*, 135716. [CrossRef]
61. Wang, B.; Gao, B.; Fang, J. Recent advances in engineered biochar productions and applications. *Crit. Rev. Environ. Sci. Technol.* **2017**, *47*, 2158–2207. [CrossRef]
62. Kumar, M.; Xiong, X.; Sun, Y.; Yu, I.K.M.; Tsang, D.C.W.; Hou, D.; Gupta, J.; Bhaskar, T.; Pandey, A. Critical Review on Biochar-Supported Catalysts for Pollutant Degradation and Sustainable Biorefinery. *Adv. Sustain. Syst.* **2020**, *4*, 1900149. [CrossRef]
63. Kumar, M.; Xiong, X.; Wan, Z.; Sun, Y.; Tsang, D.C.; Gupta, J.; Gao, B.; Cao, X.; Tang, J.; Ok, Y.S. Ball milling as a mechanochemical technology for fabrication of novel biochar nanomaterials. *Bioresour. Technol.* **2020**, *312*, 123613. [CrossRef]
64. Zheng, C.; Yang, Z.; Si, M.; Zhu, F.; Yang, W.; Zhao, F.; Shi, Y. Application of biochars in the remediation of chromium contamination: Fabrication, mechanisms, and interfering species. *J. Hazard. Mater.* **2021**, *407*, 124376. [CrossRef]
65. Zhu, Y.; Li, H.; Wu, Y.; Yin, X.-A.; Zhang, G. Effects of surface-modified biochars and activated carbon on the transformation of soil inorganic nitrogen and growth of maize under chromium stress. *Chemosphere* **2019**, *227*, 124–132. [CrossRef]
66. Ma, Y.; Liu, W.-J.; Zhang, N.; Li, Y.-S.; Jiang, H.; Sheng, G.-P. Polyethylenimine modified biochar adsorbent for hexavalent chromium removal from the aqueous solution. *Bioresour. Technol.* **2014**, *169*, 403–408. [CrossRef]
67. Nguyen, Q.A.; Kim, B.; Chung, H.Y.; Nguyen, A.Q.K.; Kim, J.; Kim, K. Reductive transformation of hexavalent chromium by ferrous ions in a frozen environment: Mechanism, kinetics, and environmental implications. *Ecotoxicol. Environ. Saf.* **2021**, *208*, 111735. [CrossRef]
68. Qiu, B.; Tao, X.; Wang, H.; Li, W.; Ding, X.; Chu, H. Biochar as a low-cost adsorbent for aqueous heavy metal removal: A review. *J. Anal. Appl. Pyrolysis* **2021**, *155*, 105081. [CrossRef]

69. Zhang, A.; Li, X.; Xing, J.; Xu, G. Adsorption of potentially toxic elements in water by modified biochar: A review. *J. Environ. Chem. Eng.* **2020**, *8*, 104196. [CrossRef]
70. Qiao, K.; Tian, W.; Bai, J.; Zhao, J.; Du, Z.; Song, T.; Chu, M.; Wang, L.; Xie, W. Synthesis of floatable magnetic iron/biochar beads for the removal of chromium from aqueous solutions. *Environ. Technol. Innov.* **2020**, *19*, 100907. [CrossRef]
71. Wu, H.; Wei, W.; Xu, C.; Meng, Y.; Bai, W.; Yang, W.; Lin, A. Polyethylene glycol-stabilized nano zero-valent iron supported by biochar for highly efficient removal of Cr(VI). *Ecotoxicol. Environ. Saf.* **2020**, *188*, 109902. [CrossRef] [PubMed]
72. Prasad, S.; Yadav, K.K.; Kumar, S.; Gupta, N.; Cabral-Pinto, M.M.; Rezania, S.; Radwan, N.; Alam, J. Chromium contamination and effect on environmental health and its remediation: A sustainable approaches. *J. Environ. Manag.* **2021**, *285*, 112174. [CrossRef] [PubMed]
73. Antoniadis, V.; Levizou, E.; Shaheen, S.M.; Ok, Y.S.; Sebastian, A.; Baum, C.; Prasad, M.N.; Wenzel, W.W.; Rinklebe, J. Trace elements in the soil-plant interface: Phytoavailability, translocation, and phytoremediation–A review. *Earth Sci. Rev.* **2017**, *171*, 621–645. [CrossRef]
74. Zhitkovich, A. Chromium in Drinking Water: Sources, Metabolism, and Cancer Risks. *Chem. Res. Toxicol.* **2011**, *24*, 1617–1629. [CrossRef]
75. Dong, X.; Ma, L.Q.; Li, Y. Characteristics and mechanisms of hexavalent chromium removal by biochar from sugar beet tailing. *J. Hazard. Mater.* **2011**, *190*, 909–915. [CrossRef] [PubMed]
76. Chakraborty, V.; Das, P. Synthesis of nano-silica-coated biochar from thermal conversion of sawdust and its application for Cr removal: Kinetic modelling using linear and nonlinear method and modelling using artificial neural network analysis. *Biomass Convers. Biorefinery* **2020**, *13*, 821–831. [CrossRef]
77. Tian, X.; Liu, M.; Iqbal, K.; Ye, W.; Chang, Y. Facile synthesis of nitrogen-doped carbon coated Fe3O4/Pd nanoparticles as a high-performance catalyst for Cr (VI) reduction. *J. Alloys Compd.* **2020**, *826*, 154059. [CrossRef]
78. Chrysochoou, M.; Theologou, E.; Bompoti, N.; Dermatas, D.; Panagiotakis, I. Occurrence, Origin and Transformation Processes of Geogenic Chromium in Soils and Sediments. *Curr. Pollut. Rep.* **2016**, *2*, 224–235. [CrossRef]
79. Frick, H.; Tardif, S.; Kandeler, E.; Holm, P.E.; Brandt, K.K. Assessment of biochar and zero-valent iron for in-situ remediation of chromated copper arsenate contaminated soil. *Sci. Total Environ.* **2019**, *655*, 414–422. [CrossRef]
80. Mahmoud, M.E.; Mohamed, A.K.; Salam, M.A. Self-decoration of N-doped graphene oxide 3-D hydrogel onto magnetic shrimp shell biochar for enhanced removal of hexavalent chromium. *J. Hazard. Mater.* **2020**, *408*, 124951. [CrossRef]
81. Shahid, M.; Shamshad, S.; Rafiq, M.; Khalid, S.; Bibi, I.; Niazi, N.K.; Dumat, C.; Rashid, M.I. Chromium speciation, bioavailability, uptake, toxicity and detoxification in soil-plant system: A review. *Chemosphere* **2017**, *178*, 513–533. [CrossRef] [PubMed]
82. Xiao, W.; Ye, X.; Yang, X.; Li, T.; Zhao, S.; Zhang, Q. Effects of alternating wetting and drying versus continuous flooding on chromium fate in paddy soils. *Ecotoxicol. Environ. Saf.* **2015**, *113*, 439–445. [CrossRef] [PubMed]
83. Ullah, A.; Kaewsichan, L.; Tohdee, K. Adsorption of hexavalent chromium onto alkali-modified biochar derived from *Lepironia articulata*: A kinetic, equilibrium, and thermodynamic study. *Water Environ. Res.* **2019**, *91*, 1433–1446. [CrossRef]
84. Maharlouei, Z.D.; Fekri, M.; Mahmoodabadi, M.; Saljooqi, A.; Hejazi, M. Chromium desorption kinetics influenced by the rice husk and almond soft husk modified biochar in a calcareous soil. *Arab. J. Geosci.* **2021**, *14*, 38. [CrossRef]
85. Shan, R.; Shi, Y.; Gu, J.; Bi, J.; Yuan, H.; Luo, B.; Chen, Y. Aqueous Cr(VI) removal by biochar derived from waste mangosteen shells: Role of pyrolysis and modification on its absorption process. *J. Environ. Chem. Eng.* **2020**, *8*, 103885. [CrossRef]
86. Liu, N.; Zhang, Y.; Xu, C.; Liu, P.; Lv, J.; Liu, Y.; Wang, Q. Removal mechanisms of aqueous Cr(VI) using apple wood biochar: A spectroscopic study. *J. Hazard. Mater.* **2020**, *384*, 121371. [CrossRef]
87. Batool, S.; Idrees, M.; Al-Wabel, M.I.; Ahmad, M.; Hina, K.; Ullah, H.; Cui, L.; Hussain, Q. Sorption of Cr(III) from aqueous media via naturally functionalized microporous biochar: Mechanistic study. *Microchem. J.* **2019**, *144*, 242–253. [CrossRef]
88. Zhang, X.; Fu, W.; Yin, Y.; Chen, Z.; Qiu, R.; Simonnot, M.-O.; Wang, X. Adsorption-reduction removal of Cr(VI) by tobacco petiole pyrolytic biochar: Batch experiment, kinetic and mechanism studies. *Bioresour. Technol.* **2018**, *268*, 149–157. [CrossRef] [PubMed]
89. Pap, S.; Bezanovic, V.; Radonic, J.; Babic, A.; Saric, S.; Adamovic, D.; Sekulic, M.T. Synthesis of highly-efficient functionalized biochars from fruit industry waste biomass for the removal of chromium and lead. *J. Mol. Liq.* **2018**, *268*, 315–325. [CrossRef]
90. Shi, Y.; Zhang, T.; Ren, H.; Kruse, A.; Cui, R. Polyethylene imine modified hydrochar adsorption for chromium (VI) and nickel (II) removal from aqueous solution. *Bioresour. Technol.* **2018**, *247*, 370–379. [CrossRef]
91. Zhao, N.; Yin, Z.; Liu, F.; Zhang, M.; Lv, Y.; Hao, Z.; Pan, G.; Zhang, J. Environmentally persistent free radicals mediated removal of Cr(VI) from highly saline water by corn straw biochars. *Bioresour. Technol.* **2018**, *260*, 294–301. [CrossRef] [PubMed]
92. Mishra, A.; Gupta, B.; Kumar, N.; Singh, R.; Varma, A.; Thakur, I.S. Synthesis of calcite-based bio-composite biochar for enhanced biosorption and detoxification of chromium Cr (VI) by *Zhihengliuella* sp. ISTPL4. *Bioresour. Technol.* **2020**, *307*, 123262. [CrossRef]
93. Matern, K.; Mansfeldt, T. Chromium Release from a COPR-Contaminated Soil at Varying Water Content and Redox Conditions. *J. Environ. Qual.* **2016**, *45*, 1259–1267. [CrossRef]
94. Xu, T.; Nan, F.; Jiang, X.; Tang, Y.; Zeng, Y.; Zhang, W.; Shi, B. Effect of soil pH on the transport, fractionation, and oxidation of chromium(III). *Ecotoxicol. Environ. Saf.* **2020**, *195*, 110459. [CrossRef]
95. Pei, G.; Zhu, Y.; Wen, J.; Pei, Y.; Li, H. Vinegar residue supported nanoscale zero-valent iron: Remediation of hexavalent chromium in soil. *Environ. Pollut.* **2019**, *256*, 113407. [CrossRef]
96. Liu, W.; Jin, L.; Xu, J.; Liu, J.; Li, Y.; Zhou, P.; Wang, C.; Dahlgren, R.A.; Wang, X. Insight into pH dependent Cr(VI) removal with magnetic Fe_3S_4. *Chem. Eng. J.* **2019**, *359*, 564–571. [CrossRef]

97. Pan, J.; Jiang, J.; Xu, R. Adsorption of Cr(III) from acidic solutions by crop straw derived biochars. *J. Environ. Sci.* **2013**, *25*, 1957–1965. [CrossRef] [PubMed]
98. Bavaresco, J.; Fink, J.R.; Rodrigues, M.L.K.; Gianello, C.; Barrón, V.; Torrent, J. Chromium Displacement in Subtropical Soils Fertilized with Hydrolysed Leather: A Laboratory Study. *Bull. Environ. Contam. Toxicol.* **2016**, *97*, 881–887. [CrossRef] [PubMed]
99. Vo, A.T.; Nguyen, V.P.; Ouakouak, A.; Nieva, A.; Doma, J.B.T.; Tran, H.N.; Chao, H.-P. Efficient Removal of Cr(VI) from Water by Biochar and Activated Carbon Prepared through Hydrothermal Carbonization and Pyrolysis: Adsorption-Coupled Reduction Mechanism. *Water* **2019**, *11*, 1164. [CrossRef]
100. Ghorbani-Khosrowshahi, S.; Behnajady, M.A. Chromium(VI) adsorption from aqueous solution by prepared biochar from *Onopordom heteracanthom*. *Int. J. Environ. Sci. Technol.* **2016**, *13*, 1803–1814. [CrossRef]
101. Ghiasi, B.; Niksokhan, M.H.; Mazdeh, A.M. Co-transport of chromium(VI) and bentonite colloidal particles in water-saturated porous media: Effect of colloid concentration, sand gradation, and flow velocity. *J. Contam. Hydrol.* **2020**, *234*, 103682. [CrossRef] [PubMed]
102. Mandal, B.K.; Vankayala, R.; Kumar, L.U. Speciation of Chromium in Soil and Sludge in the Surrounding Tannery Region, Ranipet, Tamil Nadu. *ISRN Toxicol.* **2011**, *2011*, 697980. [CrossRef]
103. He, L.; Zhong, H.; Liu, G.; Dai, Z.; Brookes, P.C.; Xu, J. Remediation of heavy metal contaminated soils by biochar: Mechanisms, potential risks and applications in China. *Environ. Pollut.* **2019**, *252*, 846–855. [CrossRef]
104. Baskar, A.V.; Bolan, N.; Hoang, S.A.; Sooriyakumar, P.; Kumar, M.; Singh, L.; Jasemizad, T.; Padhye, L.P.; Singh, G.; Vinu, A.; et al. Recovery, regeneration and sustainable management of spent adsorbents from wastewater treatment streams: A review. *Sci. Total Environ.* **2022**, *822*, 153555. [CrossRef]
105. Kozyatnyk, I.; Yacout, D.M.; Van Caneghem, J.; Jansson, S. Comparative environmental assessment of end-of-life carbonaceous water treatment adsorbents. *Bioresour. Technol.* **2020**, *302*, 122866. [CrossRef]